



Integrating aerial geophysical data in multiple-point statistics simulations to assist groundwater flow models

Neil E. M. Dickson · Jean-Christophe Comte ·
Philippe Renard · Julien A. Straubhaar ·
Jennifer M. McKinley · Ulrich Ofterdinger

Abstract The process of accounting for heterogeneity has made significant advances in statistical research, primarily in the framework of stochastic analysis and the development of multiple-point statistics (MPS). Among MPS techniques, the direct sampling (DS) method is tested to determine its ability to delineate heterogeneity from aerial magnetic data in a regional sandstone aquifer intruded by low-permeability volcanic dykes in Northern Ireland, UK. The use of two two-dimensional bivariate training images aids in creating spatial probability distributions of heterogeneities of hydrogeological interest, despite relatively ‘noisy’ magnetic data (i.e. including hydrogeologically irrelevant urban noise and regional geologic effects). These distributions are incorporated into a hierarchy system where previously published density function and upscaling methods are applied to derive regional distributions of equivalent hydraulic conductivity tensor \mathbf{K} . Several \mathbf{K} models, as determined by several stochastic realisations of MPS dyke locations, are computed within groundwater flow models and evaluated by comparing modelled heads with field observations. Results show a significant improvement in model calibration when compared to a simplistic homogeneous and isotropic aquifer

model that does not account for the dyke occurrence evidenced by airborne magnetic data. The best model is obtained when normal and reverse polarity dykes are computed separately within MPS simulations and when a probability threshold of 0.7 is applied. The presented stochastic approach also provides improvement when compared to a previously published deterministic anisotropic model based on the unprocessed (i.e. noisy) airborne magnetic data. This demonstrates the potential of coupling MPS to airborne geophysical data for regional groundwater modelling.

Keywords Aerial magnetism · Multiple-point statistics · Heterogeneity · Groundwater flow · UK

Introduction

The inherent heterogeneity of a hydrogeological system is a function of its depositional and in-situ environment, often creating highly complex structures. Distribution of hydraulic properties is therefore challenging to replicate. Heterogeneity of aquifer properties can be estimated from direct observations, requiring high measurement density (rarely available at regional scale), or can be estimated by calculating distributed equivalent values for the area of interest using sampled values (Anderson 1997; Renard and de Marsily 1997; Wen and Gómez-Hernández 1996). Use of deterministic estimations, i.e. where the system is described by interpretation of observations, can be erroneous due to uncertainties/errors in observed data, spatial correlations and human bias in interpretation. A detailed analysis into accounting for heterogeneity is delivered by de Marsily et al. (2005). Appropriate knowledge of heterogeneity is important for accurate numerical groundwater models (Chen et al. 2003). Subsurface characterization and conceptualisation is of paramount concern when creating hydrogeological models with groundwater flow components. Geostatistical and geophysical methods can assist high-resolution subsurface characterization in complementing point observations (de Marsily et al. 2005).

Received: 28 July 2014 / Accepted: 25 March 2015
Published online: 10 May 2015

© Springer-Verlag Berlin Heidelberg 2015

N. E. M. Dickson (✉) · J.-C. Comte · U. Ofterdinger
School of Planning, Architecture and Civil Engineering,
Queen’s University Belfast, David Keir Building, Belfast, Northern
Ireland, UKBT9 5AG
e-mail: ndickson03@qub.ac.uk

J.-C. Comte
School of Geosciences,
University of Aberdeen, St Mary’s Building, Old Aberdeen,
Scotland, UKAB24 3UF

P. Renard · J. A. Straubhaar
Centre d’Hydrogéologie,
Université de Neuchâtel, Emile-Argand 11, 2000, Neuchâtel,
Switzerland

J. M. McKinley
School of Geography, Archaeology and Palaeoecology,
Queen’s University Belfast, Elwood Avenue, Belfast, Northern
Ireland, UKBT7 1NN

Two-point geostatistics

The use of geostatistics (Matheron 1962, 1965) was developed for hydrogeological studies (Matheron 1967) by regarding the parameters of flow and transport equations as random functions related through stochastic partial differential equations (de Marsily 1986). According to Virdee and Kottegoda (1984), Delhomme (1978; 1979) should be credited for the application of kriging and stochastic simulations to groundwater studies. A detailed background to stochastic techniques is described in de Marsily et al. (2005), Noetinger et al. (2005) and Renard (2007). The principle of geostatistics is accounting for deterministic and random components at the same time through use of random functions. In the simplest case of a multi-Gaussian random function, the mean and covariance function are sufficient to define the heterogeneity model. In this framework, once a covariance has been inferred from field data, stochastic realizations can be created; however, this approach suffers from several limitations. It implies that the whole aquifer is statistically homogeneous and can be described with a single random function. This is not always the case, e.g. presence of aquifers and aquitards. This approach also assumes that the parameters fluctuate around a stationary or slowly varying mean (de Marsily et al. 1998), which is especially problematic when areas of high and low permeability coexist, e.g. a productive sedimentary aquifer complexly intruded by low permeability volcanics. This results in variograms showing absence of or weak spatial dependency (Dewandel et al. 2012). Several methods were developed to go beyond the traditional two point geostatistical models such as truncated pluri-Gaussian, continuous Markov chain and multiple-point statistics (MPS; Guardiano and Srivastava 1993; Strebelle 2002; Renard 2007).

Multiple-point statistics and direct sampling technique

The main limitation of all the methods based on two-point statistics such as variograms or covariances, is that they are not able to distinguish different spatial patterns especially when they are curvilinear. Strebelle (2001) showed that random fields made of lenses or channels may have variograms that are statistically identical. The two-point statistics are therefore not sufficient to describe and model realistic geological structures. Instead, if one considers the joint probability distribution of facies at multiple locations (multiple-point statistics), then one can model and reproduce complex spatial structures. In practice, these statistics are computed from a training image (TI), i.e. a conceptual model. The simulations honour conditional point data (direct observations) or secondary information such as geophysical data (Mariethoz et al. 2010). Therefore, the main advantage of MPS over standard two-point statistics is its ability to generate complex spatial features and its flexibility provided by the use of training images, which can be borrowed from a given site presenting an analogous

heterogeneity (Comunian et al. 2011). This has two main implications: using MPS, one can model more realistic patterns that will influence groundwater flow and solute transport; and one can model a broader range of different patterns by using different TI and, therefore, exploring more broadly the possible uncertainty related to aquifer heterogeneity. However, the application of MPS is dependent on the presence of a structural trend, both through a repetitive structure and this structure being accounted for in the training images, i.e. a feature should encompass several input cells. Furthermore, depending on the data input, computational burden may be significant.

Originally based on the principles of stationarity and repetitiveness (de Laco and Maggio 2011), MPS techniques have benefited from many developments allowing the user to deal with non-stationary training images (Comunian et al. 2012; de Vries et al. 2009; Mariethoz et al. 2010; Straubhaar et al. 2011). MPS has been advanced and tested for several years, e.g. three-dimensional (3D) application (Comunian et al. 2011, 2012; Michael et al. 2010), direct sampling (Mariethoz et al. 2010; Rezaee et al. 2013) and geological structure (Huysmans and Dassargues 2009; 2011; Rezaee et al. 2014), demonstrating the ability of reproducing realistic geological models in a stochastic framework, and allowing a quantification of the uncertainty.

Among the various MPS methods, the direct sampling (DS) technique (Mariethoz et al. 2010) has the advantage that it does not store the statistics inferred from the TI, which reduces computational burden. Instead, realizations are obtained by directly sampling the TI. The algorithm is described in detail in Mariethoz et al. (2010). In summary, the same steps are applied sequentially for each node x of the simulation grid: (1) the pattern $p(x)$ made up of the already simulated nodes in the neighbourhood of x is retrieved, (2) the nodes y in the TI are randomly scanned until the pattern $p(x)$ in the simulation grid and the pattern of same geometry $p(y)$ centred at y in the TI are similar, (3) then the value in the TI located at the position y is copied and pasted into the node x of the simulation grid (Fig. 1). By proceeding in such a manner, the multiple-point statistics of the TI are reproduced without having to compute them. The DS algorithm is implemented in the DeeSse software (Mariethoz et al. 2010) which requires several input parameters. The three most important are the number of neighbours within the patterns, an acceptance threshold for the discrepancy between patterns, and the maximal fraction of the TI to be scanned which influence the quality of the simulation (see Meerschman et al. 2013 for a sensitivity analysis).

MPS, geophysics and groundwater modelling

Application of DS to real data is limited in literature at present (Jha et al. 2013; Mariethoz and Renard 2010; Meerschman et al. 2014; Piroit et al. 2014) and developmental advancements are being published: bunch-pasting DS (Rezaee et al. 2013); and fast DS (Abdollahifard and Faez 2014). The work presented here explores the use of

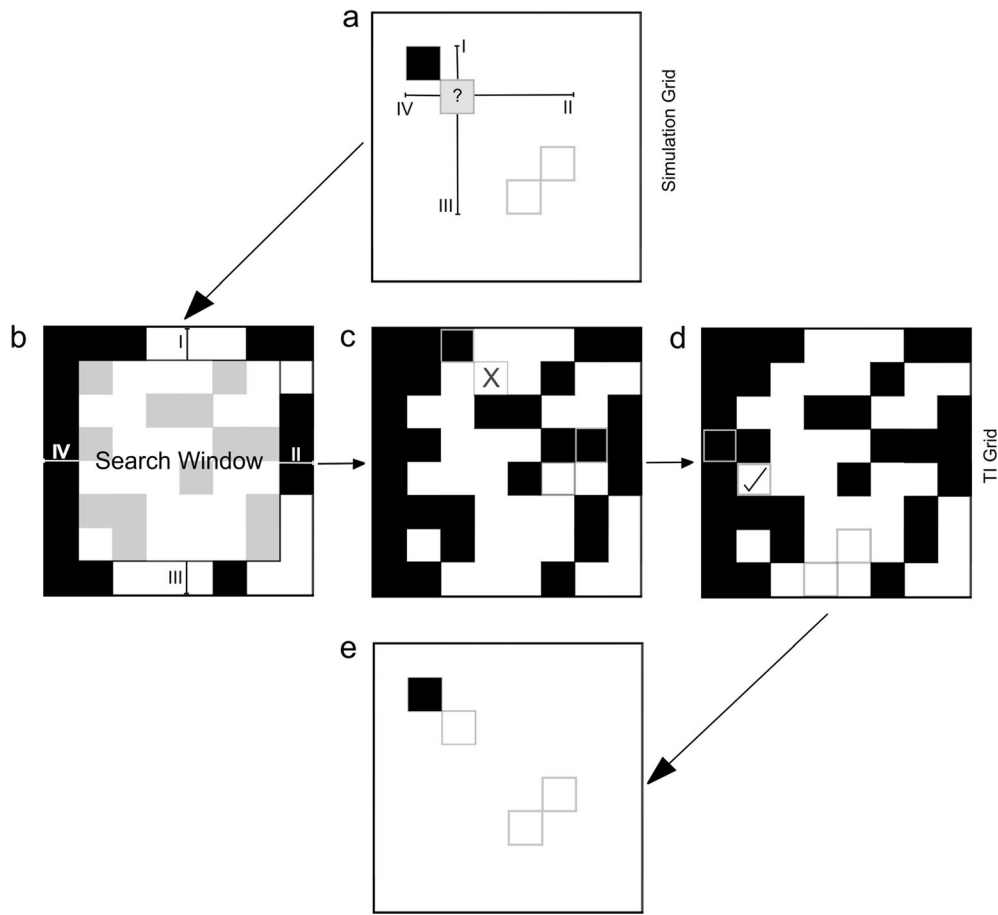


Fig. 1 Graphical illustration of the MPS direct sampling (DS) method. **a** Define the data event in the simulation grid. The *question mark* represents the node to be simulated, while the other nodes are those which have been previously simulated. **b** Define search window in the training image grid (*TI grid*). **c** Scan the search window starting from a random location. **d** The data simulation is satisfactorily matched. **e** Node now has a simulated value. Figure based on Mariethoz et al. (2010)

the DS code to determine aquifer structure through the geostatistical manipulation of aerial geophysical data (magnetics). The resulting outputs were used to derive distributions of hydraulic conductivities ultimately incorporated within numerical groundwater flow models.

Geophysics has a strong foundation in its use for subsurface hydrogeological characterization (e.g. Rubin and Hubbard 2005, and references therein). The primary use of geophysics is to provide high-resolution structural information which can assist in the spatial interpolation of point hydrogeological observations. From literature, rarely have aerial geophysics quantitatively aided the development of groundwater flow models. Examples exist that account for remote sensing (Elsheikh et al. 2011; Okazaki et al. 2011), time domain electro-magnetics (Andersen et al. 2013; Friedel et al. 2012; Gondwe et al. 2010; Rasmussen et al. 2013; Sulzbacher et al. 2012) and magnetics (Brunner et al. 2007) for a variety of applications. In this last study, Brunner et al. (2007) undertook several case studies to determine the location of faults and dykes for groundwater modelling. All studies indicated that borehole logs and groundwater level measurements were used to constrain the model. In a recent study by Dickson et al. (2014), structural information directly

derived from both ground and airborne magnetics data was used to upscale and distribute field hydraulic conductivities K , which were ultimately incorporated into regional groundwater flow models. Due to the inherent 'noise' in airborne magnetics data such as urban magnetic noise, or regional magnetic effects, alternative K distributions were provided by manual processing/smoothing of magnetics data such as homogenising geological domains. This manual interpretation gave better results, i.e. better match to groundwater observations than using the K distribution from non-interpreted magnetics data.

In this common case of 'noisy' geophysical data, MPS has the potential to be used as an alternative (stochastic) method to provide a probabilistic but 'cleaner' distribution of heterogeneities. As TIs capture known structural features of hydrogeological interest, applying MPS to geophysical data would allow the enhancement of the geophysical signal attributed to geological structures of hydrogeological influence, while avoiding the geophysical noise related to hydrogeologically irrelevant urban infrastructures and regional geological effects.

The incorporation of aerial magnetics as secondary conditioning data provides a spatial continuous input as opposed to sparse borehole data. So far, several

approaches can be used to integrate an exhaustive map of geophysical data in the MPS framework. The most frequent use is to derive facies-occurrence probability maps from the geophysical data and then to account for those probabilities during the MPS simulation process (Allard et al. 2012; Caers et al. 2003). The second approach is to invert directly the geophysical data using an MPS model as a prior distribution for the parameter field. This is currently an important area of research (Cordua et al. 2012; Hermans 2013; Hermans et al. 2014). Even if this approach is the most satisfying from a theoretical point of view, it is still hard to apply because of its high computational cost. A last alternative is to consider that the geophysical response is a secondary variable that can be directly integrated in a multivariate simulation framework as one can do with the direct sampling method. This idea was previously discussed and illustrated on synthetic examples in Mariethoz et al. (2010) or Lochbühler et al. (2014).

Consequently, the aim of this paper is to undertake a practical example of the MPS direct sampling method and explore its ability to determine aquifer heterogeneity (dyke networks intruding a sedimentary aquifer) using aerial magnetics (as a secondary variable) and, ultimately, its use to parameterize groundwater flow models. Geostatistical analysis of the aerial magnetics determines a probability spatial distribution of regionally intrusive dykes which is used as a basis for hydraulic property distribution. Hydraulic property distribution is ultimately tested within a numerical groundwater flow model by comparing model output with groundwater observations. More specifically, it is proposed to assess the potential of applying MPS-DS to airborne geophysical data in order to statistically improve the spatial resolution of dyke location (and therefore the distribution of aquifer hydraulic properties for groundwater modelling) by overcoming the noise in the input data and as an alternative to the manual processing performed by Dickson et al. (2014). It is important to emphasize that, in this study, a perfect groundwater model is not sought, rather an improved model—a model which shows improved fit to observed head data compared to a simpler conceptualization for the region. Local hydrogeological features such as springs, aquitards/heterogeneities within the sedimentary aquifer etc. are not taken into account.

Study area

Geological and hydrogeological setting

The study area is that of the Lagan Valley Aquifer in Northern Ireland (Fig. 2). Northern Ireland is a geologically complex region with bedrock geological units ranging from the Proterozoic to Cenozoic era. The Lagan Valley is a U-shaped valley, indicative of glaciation from the last glacial maximum, which is associated with the re-advancement of ice from Scotland (Fig. 2; McCabe 2008; Whitehouse et al. 2008; Wilson 1972). The residual glacial till material overlies Permo-Triassic sandstone,

namely the Sherwood Sandstone Group (SSG), which is the country's principal aquifer for industrial use and domestic supply, commonly named the Lagan Valley Aquifer. The SSG is bounded by Silurian rocks outcropping to the south-east and upland Palaeogene chalk and basalt to the north-west. The SSG overlays the Silurian metamorphic basement and dips to the north-west, underneath the basalt plateau. During the Palaeogene period, Northern Ireland was subject to two cycles of volcanic activity as the Atlantic Ocean grew apart due to rifting (Lyle 1980). This was the time when the basalt flows, composing the Antrim Plateau, were emplaced through injection of numerous dykes and sills that cut through the underlying SSG; this is now evident spanning the majority of the country, with the most northern portion analysed to be the least dense (Cooper et al. 2012; Gibson et al. 2009). Many dykes and sills were formed during a period of reverse magnetic polarity (Wilson 1959, 1970).

Most advanced interpretations of dyke emplacement have been made possible recently from aerial magnetics (AMag) data undertaken by the Tellus project, 2005–2006 (Chacksfield 2010; Cooper et al. 2012). The reduced-to-pole (RTP) and tilt derivative images account for skewness in displacement and normalize the peaks and troughs of the AMag data. The resulting image produces a varying magnetic signature across the region that reflects the varied geology. The magnetic signature of dykes disperses below the Mercia mudstone (the uppermost unit of the SSG, which has a slightly stronger magnetic signature) creating a subdued contrast between dyke and Mercia, producing 'noisy' signatures. On the Antrim Plateau, the magnetic signature is strong because of the basalt flows and results in the regional dyke signatures becoming merged with the lava flow signatures. Towards the north-west, the Palaeogene dykes trending through the SSG are effectively shown in the RTP analysis but are progressively lost due to both the dispersive effect of the Mercia and the strong signal of the overlying Antrim Lava flows (Fig. 3). In this context, MPS has a strong potential to assist in determining the dyke extent and density throughout the region despite the 'noisy' AMag data.

The Lagan Valley Aquifer has been studied for many decades (Bennett 1976; Cronin et al. 2000, 2005; Hartley 1935; Kalin and Roberts 1997; Kalin et al. 1998; Manning et al. 1970; McNeill et al. 2000; Robins 1996; Yang et al. 2004) and the region is well documented to contain Tertiary dykes. The effect of dykes on groundwater flow is acknowledged by previous authors as acting as relative barriers to flow: the hydraulic effect is described in Bennett (1976), Kalin and Roberts (1997), Burns et al. (2010), Wilson (2011) and numerous consultancy studies involving hydraulic testing. Despite those references, few (Wilson 2011; Comte et al. 2012; Dickson et al. 2014) have actually attempted to quantify both the properties of dykes and their effect at local to regional scales. Prior to the detailed multi-scale modelling works by Dickson et al. (2014), modelling studies by Cronin et al. (2000), Yang et al. (2004) and Cronin et al. (2005) mention that dykes were taken into account through compartment zonation of

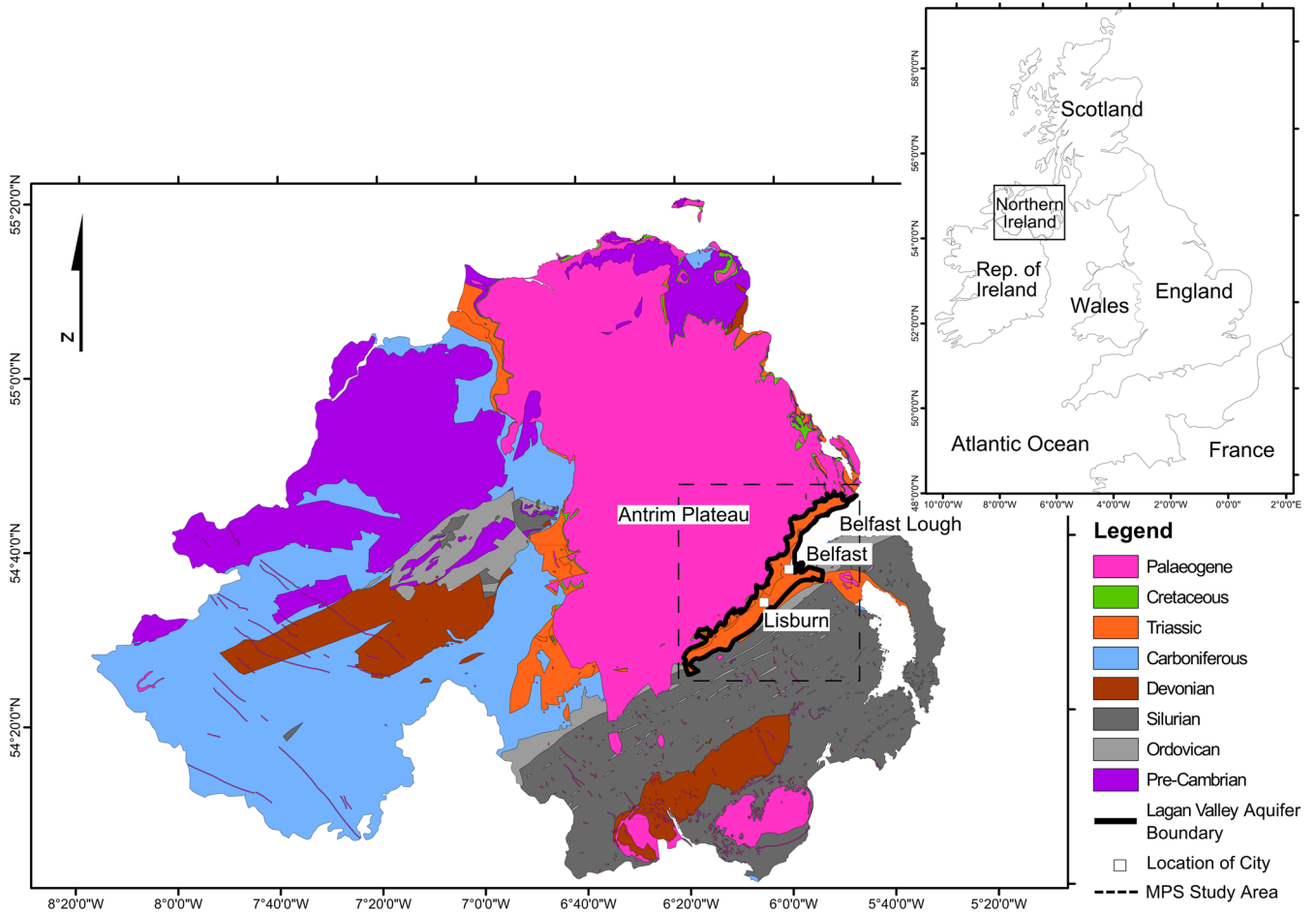


Fig. 2 A simplified geological map of Northern Ireland

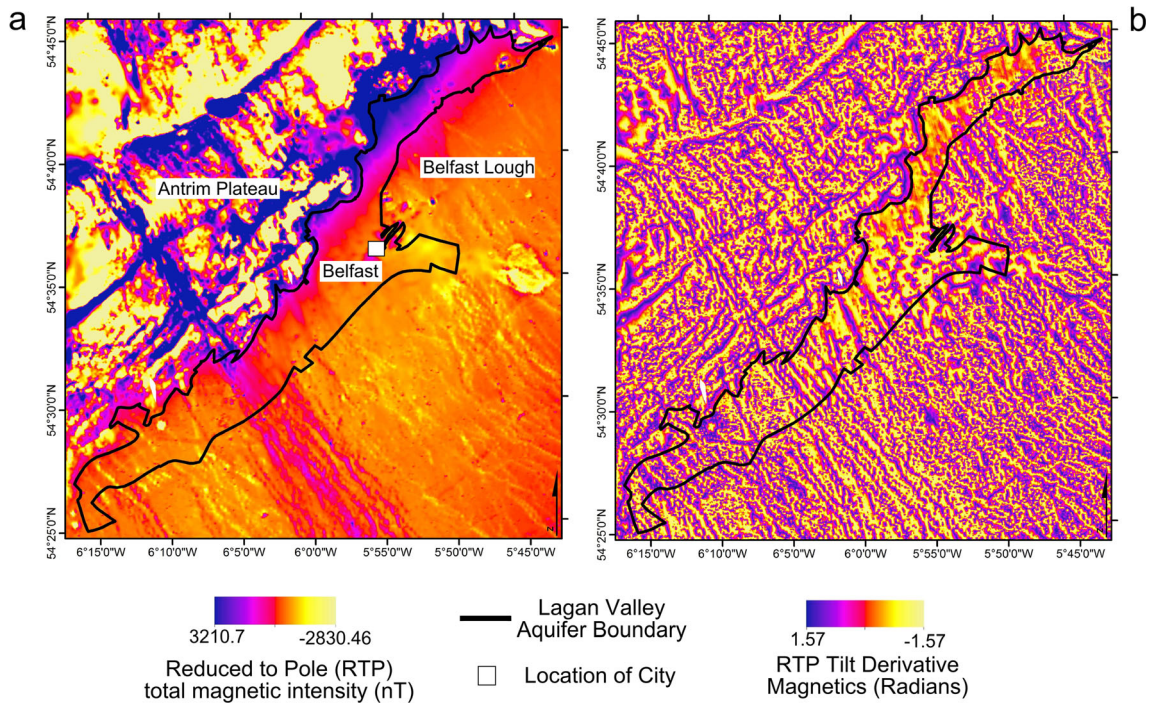


Fig. 3 Illustrations of **a** reduced-to-pole (RTP) total magnetic intensity (nT) for the area to be simulated (Lagan Valley); **b** tilt derivative of RTP aerial magnetics intensity (Radians)

the aquifer but do not describe the actual dyke properties or geometries. Yang et al. (2004) describe that model recharge was lowered over zones of high dyke densities.

Previous hydrogeological model of the Lagan Valley Aquifer

The regional aquifer was recently modelled by Dickson et al. (2014). This work has identified that the regional networks of heterogeneities (i.e. igneous intrusive dykes) can be observed as a hierarchy (Klingbeil et al. 1999), where heterogeneity observed at a small scale (i.e. field scale) can provide quantitative data regarding the properties of heterogeneities observed from a regional perspective. In the example of the Lagan Valley aquifer, it was found that heterogeneity observed from regional AMag data was the result of a cluster of several smaller field-scale dykes (each containing fractures of varying widths) whose magnetic signature was becoming merged (Burns et al. 2010; Fay et al. 2010; Dickson et al. 2014). Therefore, at the regional scale, heterogeneities were defined with equivalent hydraulic conductivities K and anisotropy properties (\mathbf{K}).

Values and distributions of \mathbf{K} tensors were estimated through a combination of upscaling and a dyke density function derived from both field and airborne data. Permeability values were obtained for field-scale dykes, the dyke fractures and the host sandstone bedrock, by in-situ measurements. Field dykes were observed to be relatively homogeneous due to an equal fracture density in its parallel and perpendicular directions, suggesting a K of $5 \times 10^{-9} \text{ m s}^{-1}$, while the sandstone value from the literature is well established at $1.2 \times 10^{-5} \text{ m s}^{-1}$. Those permeability values were upscaled to a regional scale using the model defined for banded structures by Cardwell and Parsons (1945). This model suggests that equivalent K for groundwater flow parallel and perpendicular to the banded heterogeneity trend is defined as the arithmetic (μ_a) and harmonic (μ_h) mean of individual units of K , respectively. The number of smaller heterogeneities (i.e. field-scale dykes) within a regional heterogeneity (AMag lineaments) could not be observed everywhere due to urbanization and glacial drift, so a density function was created by correlating the magnetic signature of a regional heterogeneity to the observed smaller field-scale dyke density at a number of well-known sites. The upscaling method (Cardwell and Parsons bounds) was applied to derive K parallel and K perpendicular to dyke trend (defined by an angle referred to North) throughout the region, providing therefore a \mathbf{K} tensor. The application of numerical groundwater flow models using such upscaled \mathbf{K} tensor distributions demonstrated the beneficial impact of taking into account the observed heterogeneity from airborne geophysics for regional groundwater modelling, and provided an improved aquifer conceptual model for the region than is currently accepted. However, some difficulties remained in the use of the airborne geophysical data to derive \mathbf{K} tensor distributions. Indeed, modelling results also showed that a direct use of geophysical data

was either missing or adding heterogeneities due to urban noise or regional magnetic effects. Manual processing of input \mathbf{K} tensors directly derived from geophysics such as local smoothing and homogenization, was required for the model results to better match the groundwater observations.

Methodology

MPS data preparation: training images and simulation grid

The application of MPS simulations aims in providing spatial probability distributions of dyke occurrence from the officially released AMag data (GSNI 2007). The MPS DS code used in this work was DeeSse (Mariethoz et al. 2010). Selected well-interpreted AMag regions provided the TI and simulation grid required for DeeSse. Consequently, geological features at the regional scale, i.e. dykes, could be continuously and statistically delineated while honouring the most significant geophysical structures. AMag data provided a continuous spatial input to the MPS code that does not rely solely on sparse borehole data to constrain the output. Additionally, the existing geological models provided a conceptual understanding, which was found to present an efficient input for MPS algorithms (Blouin et al. 2013; Renard 2007)

This study is not bound by complex 3D training image problems as detailed in existing literature (Blouin et al. 2013; Comunian et al. 2011, 2012), as it has been estimated through magnetic modelling at two field sites (Burns et al. 2010; Wilson 2011; Comte et al. 2012) that the dykes are sub-vertical cuboids, emplaced within the sandstone. Therefore, the spatial distribution in the Z direction was not computed and data were treated as horizontal two-dimensional (2D).

The creation of the TI was informed by previous studies of the area (Dickson et al. 2014) and from existing literature (Bennett 1976; Hartley 1935) where a general trend orientation of dyke intrusions is observed. The TI were created by digitizing existing magnetic lineaments and enlarging the resulting polyline locations to a width of 200 m wide each, as this was the average thickness observed across the region. A representative area was then chosen based on a high dyke density with repetitive structure, aiding the MPS algorithm (de Laco and Maggio 2011). To account for the varying dyke magnetic polarities (i.e. normal and reverse), three TIs were required; TI No. (TI#) 1 (Fig. 4b) accounts for normal polarity dykes; TI#2 (Fig. 4c) accounts for reverse polarity dykes; and TI#3 (Fig. 4d) contains both normal and reverse polarity dykes. TI#1 and #2 were combined after MPS simulations to determine a dataset comparable to the simulation from TI#3.

The TIs were converted into binary format with a cell size of 35 m showing only two facies: 0=sandstone and 1=dyke. In this circumstance, each dyke location is made of several cells, providing a strong presence of dykes within the TI. The boundary of the TI was also used to

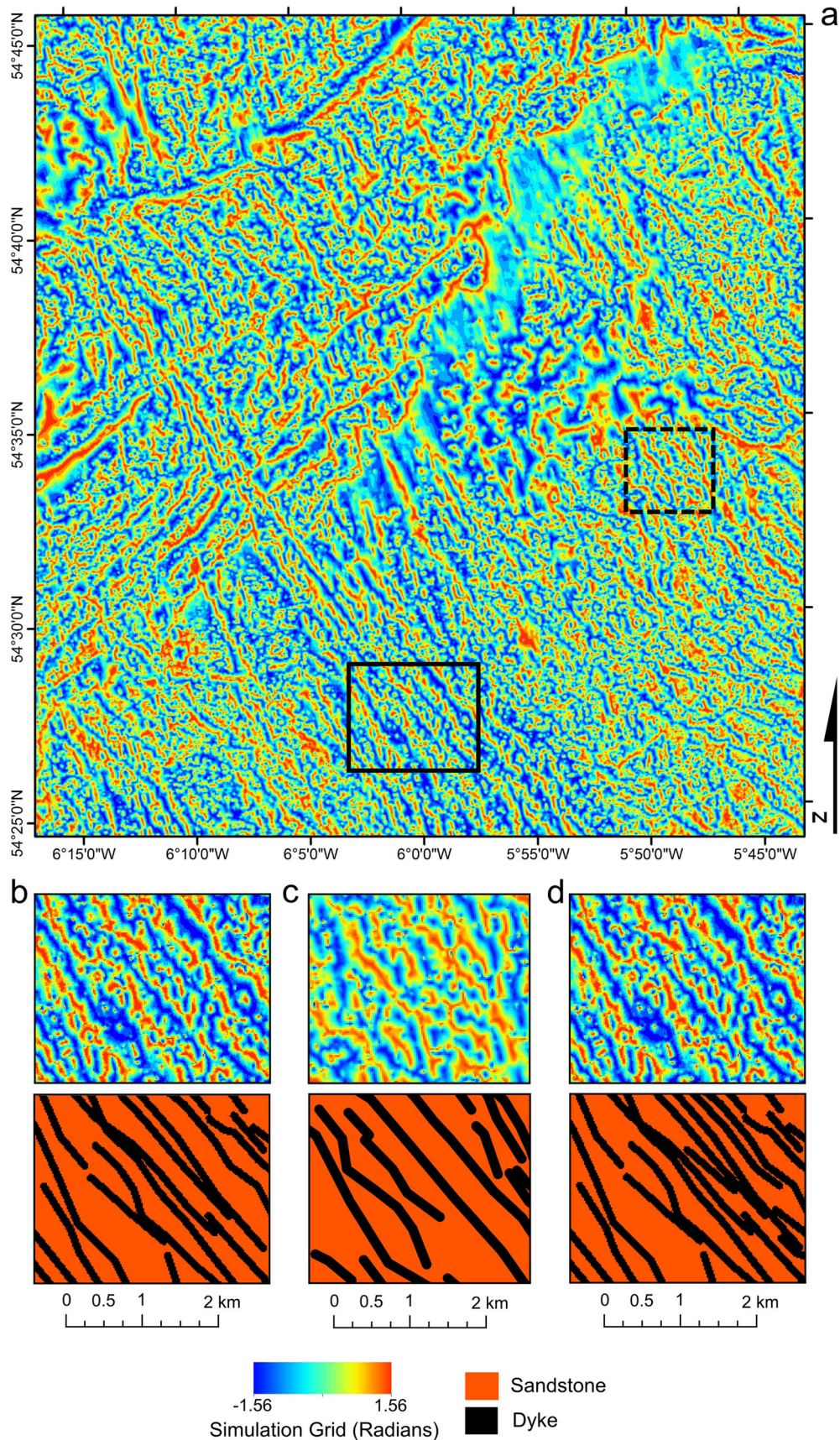


Fig. 4 Illustrations of **a** tilt derivative of reduced-to-pole (RTP) magnetics map used as input for MPS simulation grid and location of training image (TI). The *dashed-line box* represents **b** and **d**, while the *solid-line box* represents **c**. Training images: **b** normal polarity dyke TI#1; **c** reverse polarity dyke TI#2; and **d** combined normal and reverse polarity dyke TI#3

clip the magnetics data, also with a cell size of 35 m. Both the TI and clipped magnetics were converted to point data and combined to make a bivariate TI, providing continuous auxiliary data to which the binary input was compared and constrained. The normal polarity and combined polarity TIs (TI#1 and TI#3) both had a resulting grid size of $176 \times 142 \times 1$ cells ($X \times Y \times Z$), while the reverse polarity TI (TI#2) had a grid of $142 \times 128 \times 1$. The simulation grid was composed of the AMag data in point format. A grid area that covers the study area was created with a cell size of 50 m producing a resulting grid of $767 \times 786 \times 1$ cells (Fig. 4a).

MPS simulations

When running MPS simulations, a random variation of MPS parameters were considered aided by instructions detailed in Meerschman et al. (2013). A total of 6,000 simulations were generated; 3,160 for TI#1, 1,310 for TI#2 and 1,530 for TI#3. These included different neighbourhoods, acceptance thresholds and scanning fraction sizes. Analysis determined that a higher neighbourhood produced more consistent and visible dykes. The maximum neighbourhood possible was 60 due to the TI grid size, and smaller neighbours resulted in very disconnected and narrow dykes locations, the opposite to what is conceptually thought. The acceptance threshold was reduced to 0.05, implying the patterns within the training image and simulation grid had to match within 5 %.

After simulation of dyke location using the MPS, simulations with varying neighbourhoods, acceptance thresholds and fraction sizes were added (stacked) to produce one final output for each TI. Therefore the 3,160 normal (TI#1), 1,310 reverse (TI#2) and 1,530 combined (TI#3) realizations were each stacked to produce three independent maps showing the probability of dyke occurrence in each case. Stacking of MPS realizations (i.e. additive maps) was possible by using statistical software SGeMS (Remy et al. 2009). The normal and reverse polarity realisations were further combined so that the final MPS outputs were two probability maps: (1) normal and reverse polarity simulated independently, and combined afterward and (2) normal and reverse simulated together in one TI. Resulting MPS realizations are probability maps of dyke occurrence with values ranging from 0 to 100 % probability.

Probability threshold analysis

The two MPS realizations were compared to the most recent geological interpretations of geophysical data by Cooper et al. (2012) and Dickson et al. (2014). This comparison included analysis of dyke location, width and continuity. As the full-scale probability maps (ranging 0–100 % probability) provides excessive dyke occurrence throughout the region, a number of probability thresholds were tested in order to remove artefacts in a region with low probability of dyke occurrence. Tested thresholds were 50, 60, 70 and 80 % probability. For each of the two non-threshold MPS realisations, the best threshold with

regards to similarity with geological interpretation was selected to provide two additional scenarios (two threshold realisations). The four final probability maps from the two initial MPS realisations were considered for subsequent groundwater modelling.

Derivation of aquifer hydraulic conductivity tensors

Spatial distributions of regional dykes as indicated from output probability maps from the four MPS realisations were transformed to absolute magnetic values; therefore, diminishing the difference between normal and reverse polarity with a resulting range of 0–1.6 nT. The MPS probability maps were normalised to this range, in essence producing stochastic ‘cleaned’ magnetics images. These images were then used for computing hydraulic conductivity tensors (\mathbf{K}) from dyke density analysis and upscaling calculation using the method of Dickson et al. (2014). Initial K values used as input for upscaling were 5×10^{-9} and $1.2 \times 10^{-5} \text{ m s}^{-1}$ for dykes and host sandstone, respectively. In practice, a dyke density map of the region as a function of magnetic signal was first created. This map was then used for calculation of equivalent \mathbf{K} tensors by upscaling field K . This method provides values for K_1 , K_2 and K_3 data (Perpendicular to dyke trend [x , θ_i], Parallel to dyke trend [y , θ_i and z] respectively). Anisotropy angles, θ_i , were derived from orientation of MPS simulated dykes. Obtained \mathbf{K} tensors from various MPS simulations were applied as groundwater flow model inputs.

Numerical groundwater modelling

The groundwater-model geometry and boundary conditions were those from Dickson et al. (2014) to allow direct comparison of current results with previous studies. The model was created in finite element software FEFLOW 6.1 (DHI-WASY GmbH; Diersch 2002) with a relatively uniform mesh density of about 50-m spacing that reflects the elevation data distribution used for the model topography (Fig. 5). The model geometry was imported from available geological shapefiles of the SSG from the Geological Survey of Northern Ireland (GSNI).

The NW, SW and SE boundaries were assigned as no flow as this is where the SSG terminates. The NE boundary was assigned a constant head value of 0 m (sea level) as it is connected to the Irish Sea (Belfast Lough). In the literature, a groundwater divide is noted along the eastern corridor of the aquifer (Bennett 1976), so this corridor was truncated and an entering flux equal to the recharge was assigned. The recharge of the aquifer was distributed according to the distribution of the geological units and remained within the range of values provided for historical studies of the region (Manning et al. 1970; Betts 1982; Kalin and Roberts 1997): where Sherwood Sandstone outcrops it ranges from 73 to 100 mm yr^{-1} ; below the Mercia Mudstone 7– 10 mm yr^{-1} and below the basalt 4 mm yr^{-1} . Within those zones, ranges were required to account for variations in bedrock K , urbanization and glacial till cover.

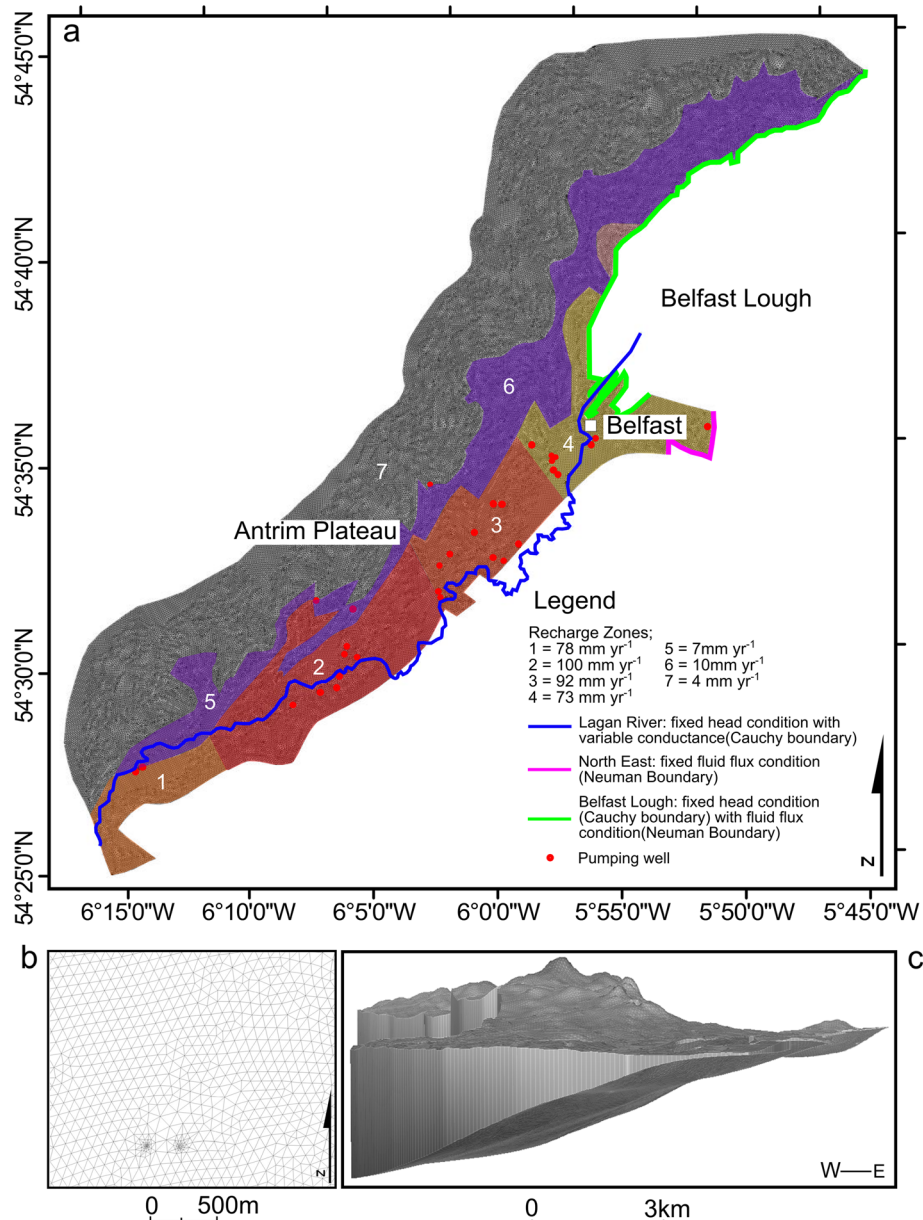


Fig. 5 Depictions of **a** model domain including boundary conditions, pumping wells and recharge zones; **b** an example of the relatively uniform mesh density which was refined for pumping wells; and **c** 3D view of the model domain illustrating the dipping nature of the Sherwood Sandstone Group

The primary river in the valley (River Lagan) was simulated by providing initial head values extracted from the digital elevation model (DEM) and applying Cauchy boundary conditions (spatially varying constant head with variable connectivity) to the adjoining nodes and element sides. The riverbed conductance varied along the length of the river to account for till and a consequential reduction of connectivity due to a thick clogging layer. Finally, groundwater abstraction rates obtained from the Northern Ireland Environment Agency (NIEA) were input as constant point fluxes (outflows).

Finally, in terms of hydraulic properties (K) parameterization, several scenarios were considered. The initial numerical model (model A) is homogeneous and isotropic

and created using typical literature values related to the region. Second, the different K tensor distributions from the four different MPS realisations provide four alternative heterogeneous and anisotropic models (models B–E). For all models, simulated heads were extracted and compared to observed monitoring data. In all, 124 observed static water levels (a composite dataset of values from literature, previous models and borehole records spanning from 1935–2011) were taken as a reference piezometry to assess the different models. Quantitative evaluation of the groundwater models was provided by calculation of the regression coefficient (r^2) and the root mean square error (RMSE) associated with the perfect fit where calculated head equals observed head (i.e. $x=y$).

Results

MPS realisations

All variations of MPS data input were used to compute the probability of occurrence of dykes (additive map E-type in geostatistical software SGeMS, Remy et al. 2009) for each type of dyke i.e. normal and reverse polarity from TI#1 and TI#2, respectively (Fig. 6a,b). This produced two images ranging between probability 0 and 1; 1 indicates that a dyke (of normal or reverse polarity depending on the map) was simulated in a cell in all circumstances, while 0 indicates a dyke was never simulated in that cell. Python script run within SGeMS permitted the combination of these two sources of information and computes a probability map by analysing pairs of simulations (one normal, one reverse) and counting within each simulation how many pixels equate to 1 in one or the other simulation and divides by the total number of simulations. The resulting image (Fig. 6c) is a probability map between 0 and 1, which accounts for both normal and reverse polarity dykes within one image. The output is very similar to existing interpretations (Cooper et al. 2012; Dickson et al. 2014) and the trend of dykes is apparent and easily seen.

In contrast, the TI that originally contained both normal and reverse polarity dykes (TI#3) produced, after MPS simulation (Fig. 6d), noisy, discontinuous dykes with a weak occurrence rate. It would appear that the dyke signatures neutralized each other, implying the code was not able to find a strong signal for each type of dyke.

As probability maps contains pixels which suggest a dyke was only simulated 20 % of the time, i.e. probability

of 0.2, probability thresholds of 50, 60, 70 and 80 % were considered to remove any anomalous or insignificant dyke simulations. The identification of the best threshold was accomplished by overlaying the simulated dyke distribution with the published studies that provide estimations to regional dyke location (Fig. 7) further verified by comparing groundwater model results with observations. The analysis of the varying probability thresholds are presented in Table 1. The threshold of 0.7, i.e. 70 % probability of dyke occurrence, was selected as it provides the closest match to published studies. Lower thresholds (60 %) produced a distribution where dykes were too thick, while higher thresholds (80 %) produced dykes that were too short and too discontinuous.

Finally the MPS realisations that have been selected and are fully presented in this paper are—model B: no probability threshold simulation of TI#3; model C: threshold of 70 % applied to TI#3 results; model D: no probability threshold simulation of TI#'s 1–2 combined; and model E: threshold of 70 % applied to TI#'s 1–2 combined results. Model A is the reference homogeneous and isotropic model. All aforementioned threshold limits were also tested within the numerical groundwater models but, for conciseness, only the final regression parameters are presented in Table 1.

Groundwater flow modelling

The homogeneous and isotropic model (model A) and the four alternative distributed **K** models (models B–E) derived from MPS realisations using the upscaling

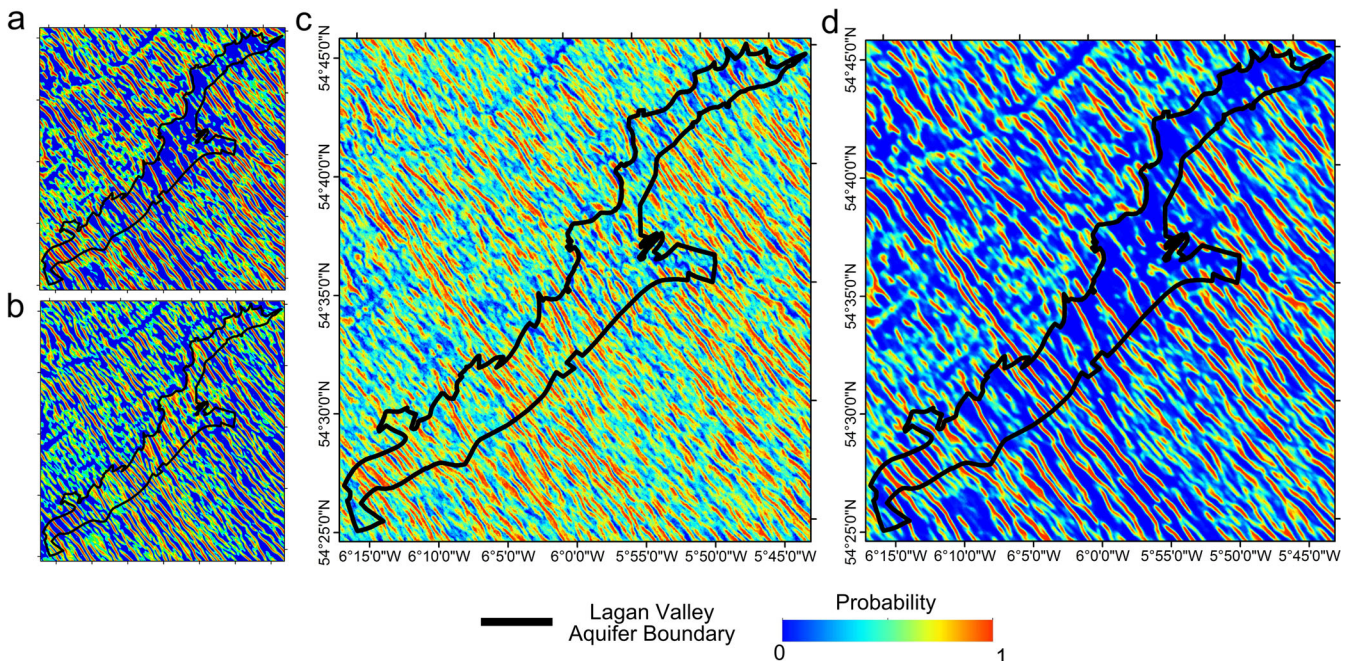


Fig. 6 Maps showing E-type image of MPS realisations from normal and reverse polarity dykes computed independently or together; **a** realisation from normal polarity TI#1; **b** realisation from reverse polarity TI#2; **c** the two previous E-type realisations combined and **d** realisation from combined normal and reverse polarity TI#3

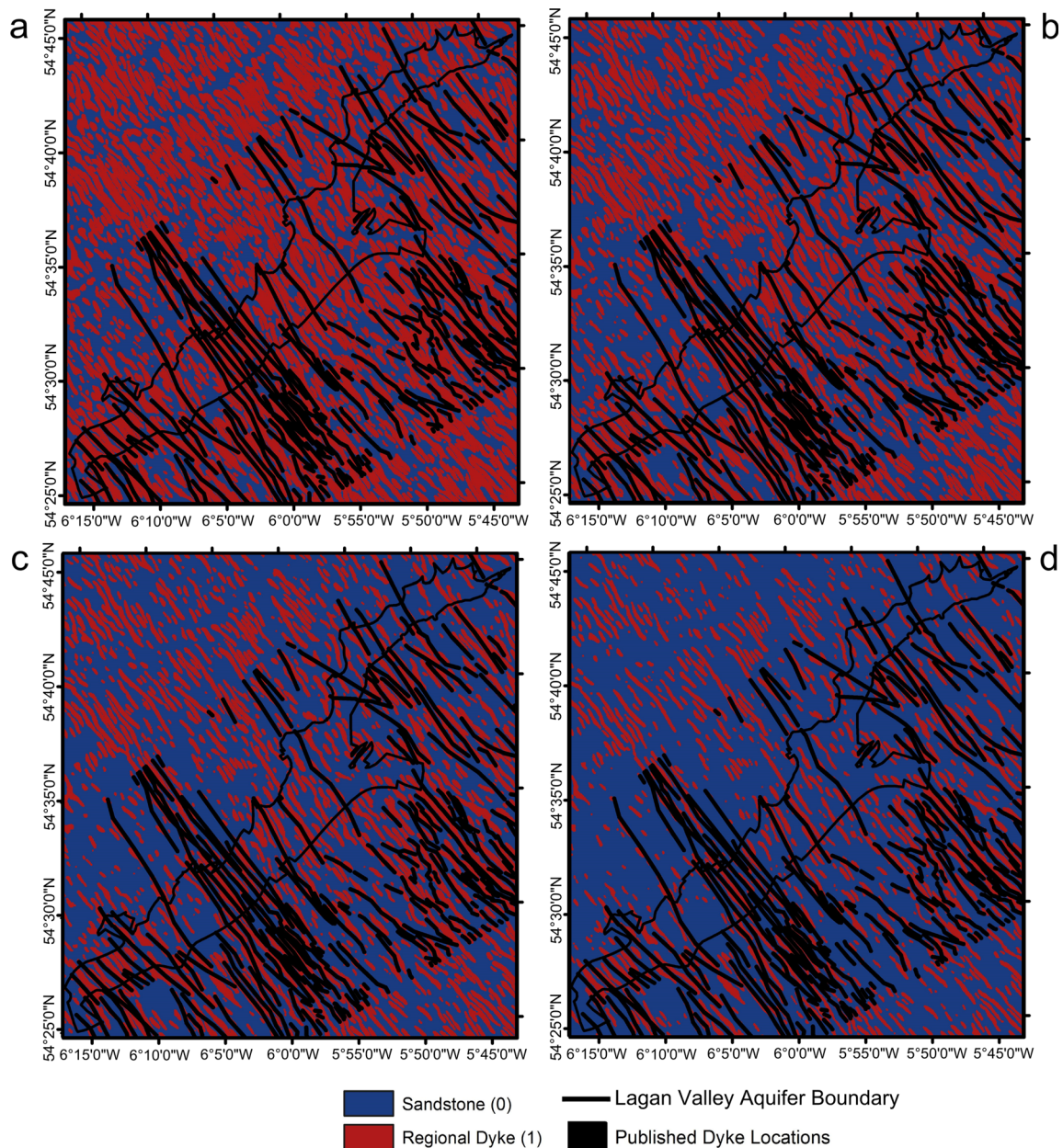


Fig. 7 Illustrations depicting the MPS realizations throughout the region for different probability thresholds and when normal and reverse polarity dykes are input independently (TI#'s 1–2). **a** Threshold of 50 %; **b** threshold of 60 %; **c** threshold of 70 %; and **d** threshold of 80 %. *Black lines* are representative of interpreted regional dyke locations from published literature (Cooper et al. 2012; Dickson et al. 2014). Images indicate that a low percentage threshold overestimates dyke occurrence, while a higher threshold underestimated dyke occurrence and produce too thin, discontinuous dykes. From image **c**, 70 % is chosen as the best match to published sources

technique of Dickson et al. (2014) were used to compute groundwater flow in the SSG aquifer. Figure 8 illustrates the dyke density map and \mathbf{K} distribution derived from MPS simulations where normal and reverse dyke signatures are computed independently in MPS simulations (TI#'s 1–2) before combining, together with subsequent application of the probability threshold of 0.7 (model E). The inclusion of lower \mathbf{K} heterogeneity features alters the groundwater flow when compared to the reference model (model A). All groundwater model results are presented in Fig. 9 and Table 1.

The homogeneous and isotropic model (model A), which was built using literature values known for the region and which contains no heterogeneity, has a r^2 and RMSE of 0.68 and 8.68 m respectively. In general, as observed from Fig. 9, the groundwater head elevations are underestimated during simulation, especially in areas of highest head levels, i.e. the areas of observed high dyke density. The region that is close to Belfast Lough (with constant head condition) is well constrained and shows a good fit to observations.

Results obtained for model B (TI#3, no threshold) suggest a poor correlation with a relatively low r^2 of 0.67

Table 1 Groundwater model calibration statistics (r^2 and $RMSE$) for the different MPS realisations (from separated or combined training images) and for different probability thresholds of 50, 60, 70 and 80 %. Groundwater models *A–E* are also indicated

MPS realization	Groundwater model	Regression coefficient (r^2)	Root mean square error (RMSE)
Isotropic	Model A	0.69	8.86 m
No threshold TI#’s 1–2	Model D	0.45	29.60 m
TI#’s 1–2 (50 % threshold)	Not presented	0.78	10.00 m
TI#’s 1–2 (60 % threshold)	Not presented	0.80	8.88 m
TI#’s 1–2 (70 % threshold)	Model E	0.87	6.77 m
TII#’s 1–2 (80 % threshold)	Not presented	0.77	8.17 m
No threshold TI#3	Model B	0.67	17.06 m
TI#3 (50 % threshold)	Not presented	0.71	11.21 m
TI#3 (60 % threshold)	Not presented	0.73	8.57 m
TI#3 (70 % threshold)	Model C	0.79	7.40 m
TI#3 (80 % threshold)	Not presented	0.72	8.23 m

and a high RMSE of 17.02 m. The inaccurate simulation was expected due to all probabilities of heterogeneity being included, creating anisotropy and variation in the flow regime when it was not appropriate to do so. All levels of heterogeneity probability influenced the **K**, particularly **K** perpendicular, slowing the groundwater flow. This has resulted in simulated head generally much higher than observations.

Model C (TI#3, threshold 0.7) produces calculated heads with a relatively significant r^2 (0.79) and a low RMSE (7.88 m). This model is significantly better than the direct model. The significant improvement in regression compared to model A is attributed to the inclusion of the dykes which are acting like barriers, allowing groundwater to build up. This is especially true in the center of the valley, away from constrained head values and also the location of a dense band of regional heterogeneity. The large-scale heterogeneity permitted compartmentalization and alteration of flow, creating a closer match to observed head levels. However, the higher observed groundwater heads are underestimated by the simulations. A component of heterogeneity is missing in upgradient aquifer regions, underestimating the compartmentalization of the groundwater. This is due to TI#3 producing fewer dykes throughout the region due to the MPS DS code not suitably separating adjacent reverse and normal polarities.

Model D (TI#’s 1–2, no threshold) provides a very poor correlation to observed head values, even lower than model B. By retaining all probabilities of dyke occurrence, it is producing too large an anisotropy effect resulting in most of groundwater head elevations being overestimated (r^2 of 0.4 and RMSE of 29.58 m). Model B also performs badly due to the increased number of heterogeneities present which results from the method of combining the probabilities of positive and reverse polarity after MPS computation of the independent training images. The input for model D contained a strong presence and larger number of heterogeneities, which has had an overestimating impact on the groundwater flow.

Lastly, model E (TI#’s 1–2, threshold 0.7) produces the best model fit with an r^2 of 0.87 and RMSE of 6.77 m. In this case, the model keeps the large number of simulated heterogeneities resulting from computing independently

normal and reverse polarity dykes (TI#’s 1–2) in MPS simulations, while removing the less significant probabilities of heterogeneities under 70 %. It provides an improvement when compared to model C in simulating higher heads in upgradient aquifer regions.

Discussion

In previous results of Dickson et al. (2014), a modelled **K** distribution directly derived from unprocessed airborne magnetic data (deterministic approach by contrast with the MPS stochastic approach) produced an r^2 and RMSE of 0.83 and 7.07 m respectively. In this work, the best model using **K** distribution from MPS realisations shows an improved fit of r^2 of 0.87 and RMSE of 6.77 m. Figure 10 presents the comparison of both model results. The better results obtained with application of MPS are due to the MPS realisations being well constrained by the conceptual information of the TIs allowing correction of hydrogeologically irrelevant magnetic signal, i.e. ‘noise’. MPS realisations produced more continuous dykes where the magnetic data are blurred by urban noise, while effectively reproducing dykes in areas of strong, unambiguous magnetic signatures. They also avoided the creation of heterogeneities in areas affected by regional magnetic effects such as the north-west border, close to the Antrim Plateau lava flows. As a result, the integration of the MPS results provides a more comprehensive average of dyke occurrences and more continuous dykes which increase their effect on groundwater flow and generally results in a higher water table. The MPS method provides added value to the deterministic method of Dickson et al. (2014) providing a statistical implementation of dyke location useful in locations which are obscured by noise in the airborne data.

However, this has mainly been feasible due to the two different TI used and with application of a probability threshold of 0.7 to MPS outputs. A combined TI which shows both normal and reverse polarity dykes produces simulations with not as strong a probability of occurrence and not as dense. By simulating the normal and reverse polarity dykes separately, the MPS DS code can more

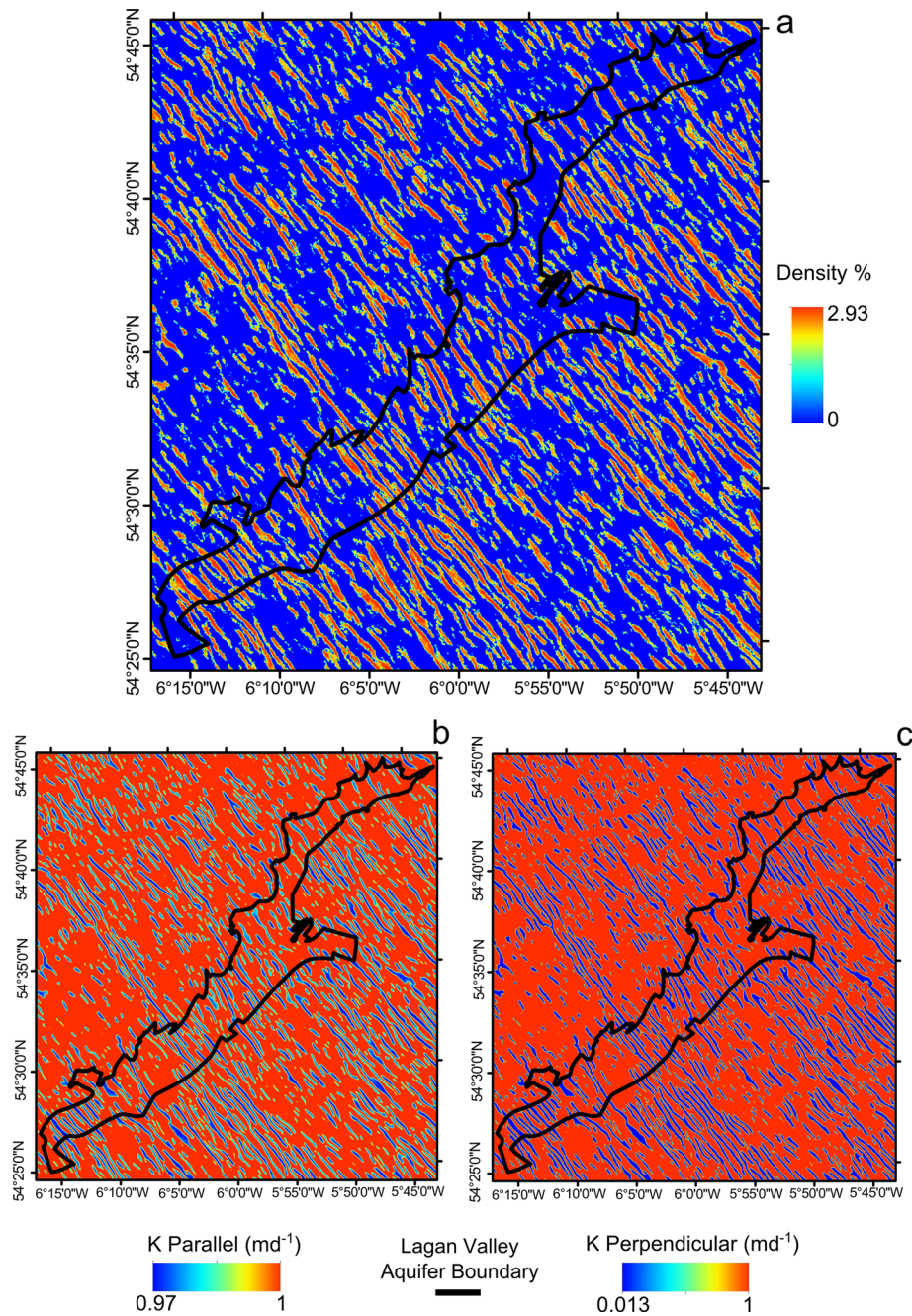


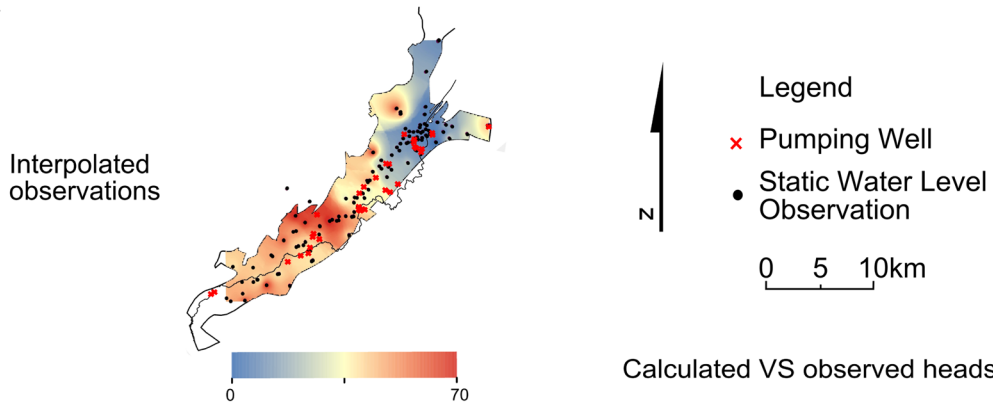
Fig. 8 Spatial computation of dyke density and hydraulic conductivity using the upscaling method of Dickson et al. (2014): **a** calculated dyke density throughout the region using the normalized magnetic prediction from the MPS probability realisations; **b** parallel K calculated from density map; and **c** perpendicular K calculated from density map. Here is the case where normal and reverse polarity dykes (TI#1 and TI#2) are computed independently in MPS and a probability threshold of 0.7 is applied to the combined results (model E)

effectively distinguish the relationships and trends between the magnetics and TI.

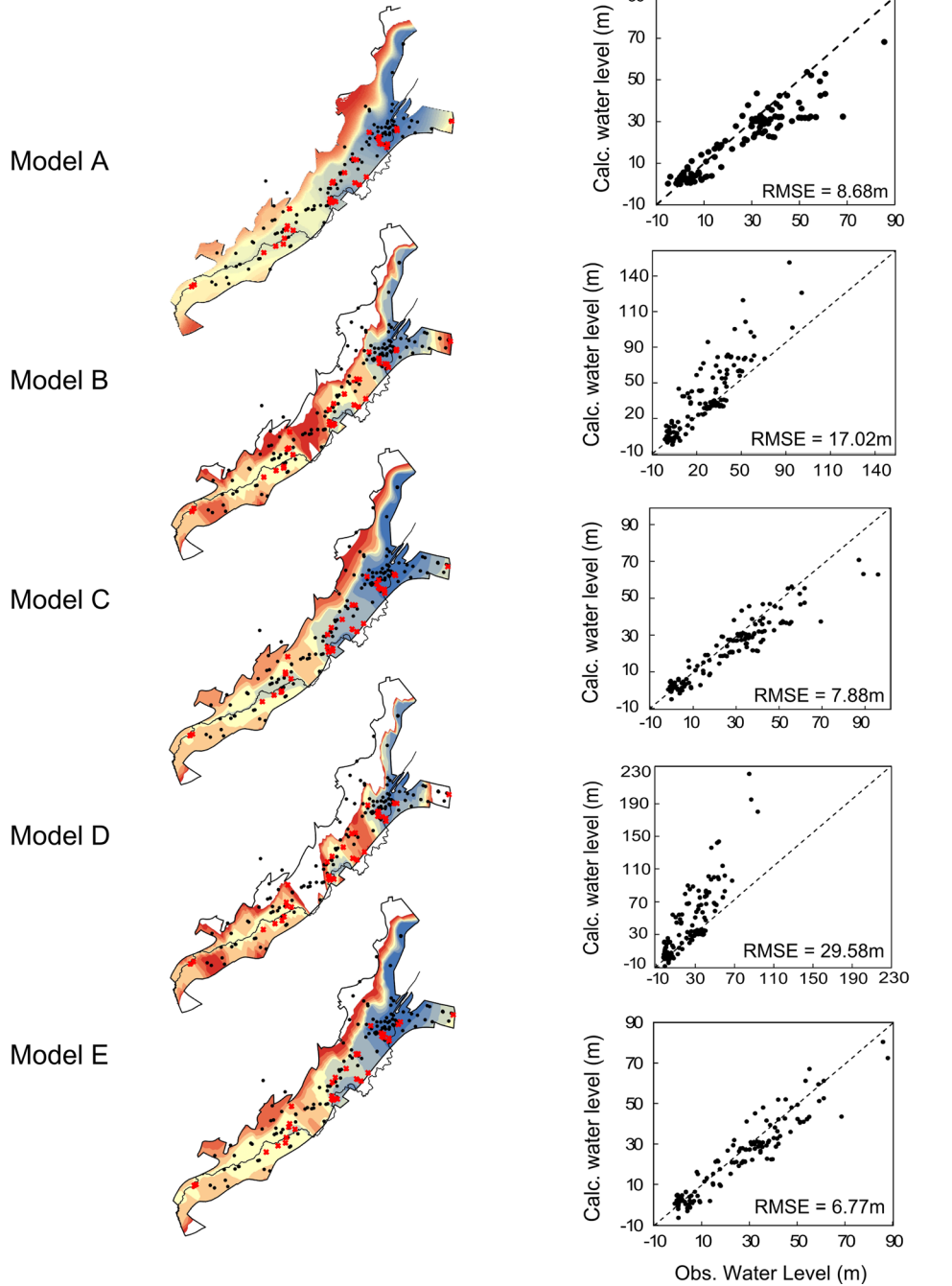
Overall, the resulting groundwater flow models confirm the benefit of including regional heterogeneity. When calibrated to geophysical observations, MPS realisations assist the parameterization of groundwater models. The continuous regional input geophysical data in conjunction with MPS analysis, allows for a well-constrained aquifer conceptual model.

This study provides an additional analysis component compared to existing sources (Huysmans and Dassargues 2009; Rezaee et al. 2014) who relied upon point information from boreholes. Information can be extrapolated from such sources; however, this is generally accompanied by high amounts of uncertainty and error. With the acquisition of continuous data from various geophysical sources, it can provide a continuous bivariate input which, as demonstrated, aids model calibration and output.

a



b



◀ **Fig. 9** Maps of **a** observed groundwater heads and **b** simulated groundwater heads (m msl), throughout the Lagan Valley aquifer for each of the five **K** models (*A–E*). Model regression is provided to show the fit of the models alongside the *RMSE* values

Conclusions and further study

The implementation of MPS DS approach has been efficient with regards to heterogeneity simulation. The ability to input a bivariate and continuous TI alongside

the flexibility within the code (pattern size, threshold, scanning fraction) allow many equally probable realisations of heterogeneity occurrence. For this study, the trending dyke locations were approximately known and the MPS simulations have confirmed their location, while also providing additional locations due to the statistical nature of the code, not prone to human bias.

The conjunctive analysis of airborne magnetics data with MPS, has provided alternative structural models to the current

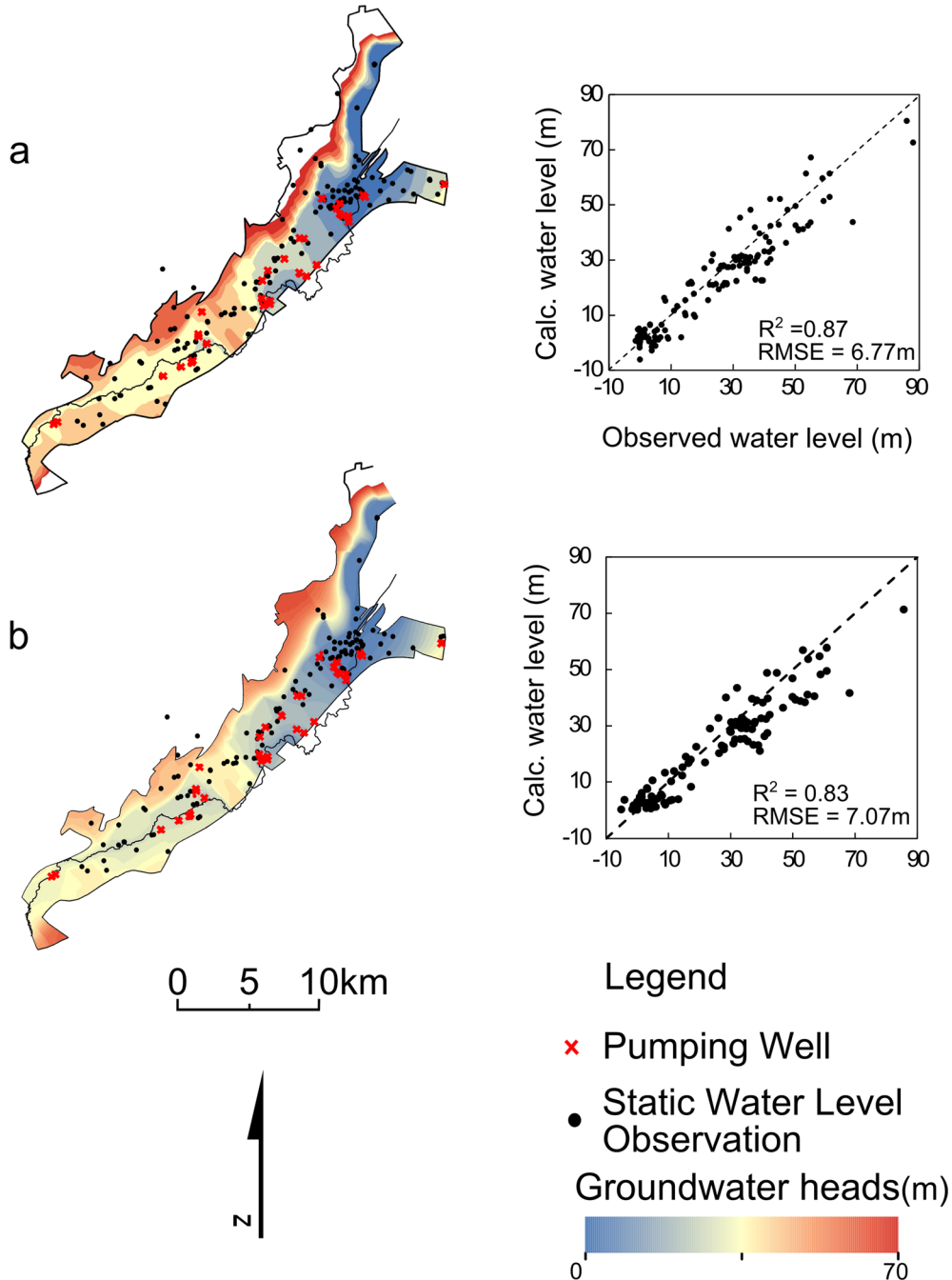


Fig. 10 Comparison of results obtained from the best groundwater model with previous results of Dickson et al. (2014): **a** best groundwater model results (*model E*) using MPS realisations obtained from two separated magnetics training images TI#1 and TI#2 and with application of a probability threshold of 0.7; **b** groundwater model results from Dickson et al. (2014) using directly the unprocessed/uninterpreted magnetics data

understanding of flow throughout the Lagan Valley aquifer. The addition of this statistical anisotropy drastically alters the flow vectors and water potential throughout this region, which improves previous work by Dickson et al. (2014), where magnetic data were incorporated directly with noise and hydrogeologically irrelevant magnetic signatures. Thanks to the use of interpreted TIs, the application of MPS to airborne magnetics data allows one to enhance the magnetic heterogeneities of hydrogeological relevance. This significantly improves the resulting groundwater models.

However, raw computation of MPS realizations (full range of probability maps of dyke occurrence) do not provide the best results, both when MPS realisations are compared to existing geological interpretations and when groundwater simulations are compared to observations. This is due to the computation of heterogeneities with low probability of occurrence. Instead, the best models (both MPS realizations and groundwater simulations) are obtained when a probability threshold of 70 % is applied, i.e. when only heterogeneities with a probability of occurrence higher than 70 % are computed. Moreover, for those threshold models, the best results are obtained when the training images for normal and reverse magnetic polarity dykes are used independently, i.e. input as separate TIs and combined after simulation via MPS code.

It is suggested that any future modelling of the region should be undertaken in transient mode (if water level data is available) and should include local features, e.g. springs. Moreover, if the dyke thickness varied or the orientation was variable, it is unclear how well the MPS code would perform in the assessment of dyke distribution. The method presented here could be extended to a more diverse TI with additional facies included. The ability to use a bivariate continuous TI greatly constrains the MPS simulations. The thousands of simulations were run sequentially with different parameters able to be simulated at the same time using different cores of the computer, therefore increasing simulation time, although it did provide a high CPU burden. The methodology used here could be applied to an alternative more-complex geology or to a smaller study area, perhaps negating the need for upscaling. However, the high-resolution geophysics would be a necessity.

Acknowledgements Neil Dickson was funded through a PhD studentship in Queen's University, Belfast, from the Northern Irish Department of Education and Learning (DEL). We acknowledge two anonymous reviewers as well as the associate editor A. McDonald and the editor E. Screaton for valuable comments that contributed to improving the final manuscript.

References

- Abdollahifard MJ, Faez K (2014) Fast direct sampling for multiple-point stochastic simulation. *Arab J Geosci* 7:1927–1939. doi:10.1007/s12517-013-0850-4
- Allard D, Comunian A, Renard P (2012) Probability aggregation methods in geoscience. *Math Geosci* 44(5):545–581. doi:10.1007/s11004-012-9396-3
- Anderson MP (1997) Characterization of geological heterogeneity. In: Dagan G, Neuman SP (eds) *Subsurface flow and transport: a stochastic approach*. Cambridge University Press, New York, pp 23–43

- Andersen TR, Poulsen SE, Christensen S, Jørgensen F (2013) A synthetic study of geophysics-based modelling of groundwater flow in catchments with a buried valley. *Hydrogeol J* 21:491–503. doi:10.1007/s10040-012-0924-5
- Bennett JRP (1976) *The Lagan Valley: hydrogeological study*. Open File Report 57, Geological Survey of Northern Ireland, Belfast
- Betts NL (1982) Synoptic climatology of Northern Ireland, chapter 1. In: Cruickshank JG, Wilcox DN (eds) *Northern Ireland: environment and natural resources*. The Queen's University of Belfast, University Road, Belfast, Northern Ireland, pp 9–42
- Blouin M, Martel R, Gloaguen E (2013) Accounting for aquifer heterogeneity from geological data to management tools. *Groundwater* 51(3):421–431. doi:10.1111/j.1745-6584.2012.00982.x
- Brunner P, Hendricks Franssen H-J, Kogthang L, Bauer-Gottwein P, Kinzelbach W (2007) How can remote sensing contribute in groundwater modelling? *Hydrogeol J* 15:5–18. doi:10.1007/s10040-006-0127-z
- Burns C, Comte J-C, Gaffney L, Ofterdinger U, Young M (2010) Characterization of the effect of dyke swarms on groundwater flow in a sedimentary coastal aquifer by combined geophysical and hydrogeological modelling. Paper presented at American Geophysical Union, Fall Meeting 2010, San Francisco, Abstract no. H11E-0842, AGU, Washington, DC
- Caers J, Strebelle S, Payrazyan K (2003) Stochastic integration of seismic data and geologic scenarios: a West Africa submarine channel saga. *Lead Edge* 22(3):192–196
- Cardwell WT, Parsons RL (1945) Average permeabilities of heterogeneous oil sands. *Trans Am Inst Min Metall Pet Eng* 160(1):34–42. doi:10.2118/945034-G
- Chacksfield BC (2010) A preliminary interpretation of Tellus airborne magnetic and electromagnetic data for Northern Ireland, British Geological Survey Internal Report, IR/07/041, BGS, Nottingham, UK, 51 pp
- Chen Y, Durlofsky LJ, Gerritsen M, Weh XH (2003) A coupled local-global upscaling approach for simulating flow in highly heterogeneous formations. *Adv Water Resour* 26:1041–1060. doi:10.1016/S0309-1708(03)00101-5
- Comte J-C, Ofterdinger U, Wilson C, Burns C (2012) Role hydrogéologique des dykes volcaniques au sein de l'aquifère cotier des grès de Belfast (Irlande du Nord) et implications pour la gestion de la ressource [Hydrogeological role of volcanic dykes in the coastal sandstone aquifer of Belfast (Northern Ireland) and implications for the management of resources]. Paper presented at the Dix-huitièmes journées techniques du Comité Français d'Hydrogéologie de l'Association Internationale des Hydrogéologues, Ressources et gestion des aquifères littoraux, Cassis, France, March 2012
- Comunian A, Renard P, Straubhaar J, Bayer P (2011) Three-dimensional high resolution fluvio-glacial aquifer analog, part 2: geostatistical modeling. *J Hydrol* 405:10–23. doi:10.1016/j.jhydrol.2011.03.037
- Comunian A, Renard P, Straubhaar J (2012) 3D multiple-point statistics simulation using 2D training images. *Comput Geosci* 40:49–65. doi:10.1016/j.cageo.2011.07.009
- Cooper MR, Anderson H, Walsh JJ, Van Dam CL, Young ME, Earls G, Walker A (2012) Palaeogene Alpine tectonics and Icelandic plume-related magmatism and deformation in Northern Ireland. *J Geol Soc Lond* 169:29–36. doi:10.1144/0016-76492010-182
- Cordua KS, Hansen TM, Mosegaard K (2012) Monte Carlo full-waveform inversion of crosshole GPR data using multiple-point geostatistical a priori information. *Geophysics* 77(2):H19–H31. doi:10.1190/geo2011-0170.1
- Cronin AA, Elliot T, Yang Y, Kalin RM (2000) Geochemical modelling and isotope studies in the Sherwood Sandstone Aquifer, Lagan Valley, Northern Ireland. In: Dassargues A (ed) *Tracers and modelling in hydrogeology*. IAHS, Oxfordshire, UK, pp 425–432
- Cronin AA, Barth JAC, Elliot T, Kalin RM (2005) Recharge velocity and geochemical evolution for the Permo-Triassic

- Sherwood Sandstone, Northern Ireland. *J Hydrol* 315:308–324. doi:10.1016/j.jhydrol.2005.04.016
- de Laco S, Maggio S (2011) Validation techniques for geological patterns simulations based on variogram and multiple-point statistics. *Math Geosci* 43:483–500. doi:10.1007/s11004-011-9326-9
- de Marsily G (1986) Quantitative hydrogeology: groundwater hydrology for engineers. Academic, London
- de Marsily G, Delay F, Teles V, Schafmeister MT (1998) Some current methods to represent the heterogeneity of natural media in hydrogeology. *Hydrogeol J* 6:115–130
- de Marsily G, Delay F, Gonçalves J, Renard P, Teles V, Violette S (2005) Dealing with spatial heterogeneity. *Hydrogeol J* 13:161–183. doi:10.1007/s10040-004-0432-3
- de Vries LM, Carrera J, Falivene O, Gratacós O, Slooten LJ (2009) Application of multiple point geostatistics to non-stationary images. *Math Geosci* 41:29–42. doi:10.1007/s11004-008-9188-y
- Delhomme JP (1978) Kriging in the hydrosociences. *Adv Water Resour* 1(5):251–266. doi:10.1016/0309-1708(78)90039-8
- Delhomme JP (1979) Spatial variability and uncertainty in groundwater flow parameters: a geostatistical approach. *Water Resour Res* 15(2):269–280. doi:10.1029/WR015i002p00269
- Dewandel B, Maréchal JC, Bour O, Ladouche B, Ahmed S, Chandra S, Pauwels H (2012) Upscaling and regionalizing K and effective porosity at watershed scale in deeply weathered crystalline aquifers. *J Hydrol* 416–417:83–97. doi:10.1016/j.jhydrol.2011.11.038
- Dickson NEM, Comte J-C, McKinley JM, Ofterdinger US (2014) Coupling ground and airborne geophysical data with upscaling techniques for regional groundwater modelling of heterogeneous aquifers: case study of a sedimentary aquifer intruded by volcanic dykes in Northern Ireland. *Water Resour Res* 50(10):7984–8001. doi:10.1002/2014WR015320
- Diersch HJG (2002) FEFLOW reference manual. Wasy GmbH, Institute for Water Resources Planning and Systems Research, Berlin
- Elsheikh A, Abdelsalam MG, Mickus K (2011) Geology and geophysics of the West Nubian Paleolake and the Northern Darfur Megalake (WNPL-NDML): implication for groundwater resources in Darfur, northwestern Sudan. *J Afr Earth Sci* 61:82–93. doi:10.1016/j.jafrearsci.2011.05.004
- Fay DQM, Young ME, Walker ASD (2010) Ground magnetometer survey of dykes in Co. Down. Paper presented at 53rd Irish Geological Research Meeting (IGRM) Ulster Museum, Belfast
- Friedel MJ, de Souza Filho OA, Iwashita F, Silva AM, Yoshinaga S (2012) Data-driven modeling for groundwater exploration in fractured crystalline terrain, northeast Brazil. *Hydrogeol J* 20:1061–1080. doi:10.1007/s10040-012-0855-1
- Gibson PJ, Lyle P, Thomas N (2009) Magnetic characteristics of the Cuilcagh dykes, Co. Fermanagh, Northern Ireland. *Ir J Earth Sci* 27:1–9. doi:10.3318/IJES.2009.27.1
- Gondwe BRN, Lerer S, Stisen S, Marín L, Rebolledo-Vieyra M, Merediz-Alonso G, Bauer-Gottwein P (2010) Hydrogeology of the south-eastern Yucatan Peninsula: new insights from water level measurements, geochemistry, geophysics and remote sensing. *J Hydrol* 389:1–17. doi:10.1016/j.jhydrol.2010.04.044
- GSNI (2007) TELLUS airborne magnetic maps. Geological Survey of Northern Ireland, Belfast
- Guardiano FB, Srivastava RM (1993) Multivariate geostatistics: beyond bivariate moments. In: Soares A (ed) *Geostatistics: Troia '92*, vol 1. Kluwer, Dordrecht, The Netherlands, pp 133–144
- Hartley JJ (1935) The underground water resources of Northern Ireland. Institution of Civil Engineers, Belfast
- Hermans TJ (2013) Integration of near-surface geophysical, geological and hydrogeological data with multiple-point geostatistics in alluvial aquifers. Faculty of Applied Sciences, Univ. Of Liege, Belgium
- Hermans T, Caers J, Nguyen F (2014) Assessing the probability of training image-based geological scenario using geophysical data. In: Pardo-Iguzquiza E, Gaurdiola-Albert C, Heredia J, Moreno-Merino L, Dura JJ, Vargas-Guzman JA (eds) *Mathematics of planet Earth: proceedings of the 15th Annual Meeting of the International Association for Mathematical Geosciences*. Springer, New York, pp 679–682
- Huysmans M, Dassargues A (2009) Application of multiple-point geostatistics on modelling groundwater flow and transport in a cross-bedded aquifer (Belgium). *Hydrogeol J* 17:1901–1911. doi:10.1007/s10040-009-0495-2
- Huysmans M, Darrargues A (2011) Direct multiple-point geostatistical simulation of edge properties for modeling thin irregularly shaped surfaces. *Math Geosci* 43:521–536. doi:10.1007/s11004-011-9336-7
- Jha SK, Mariethoz G, Kelly BFG (2013) Bathymetry fusion using multiple-point geostatistics: novelty and challenges in representing non-stationary bedforms. *Environ Model Softw* 50:66–76. doi:10.1016/j.envsoft.2013.09.001
- Kalin RM, Roberts C (1997) Groundwater Resources in the Lagan Valley Sandstone Aquifer, Northern Ireland. *JCIWEM* 11:133–139
- Kalin R, Yang Y, Cronin A (1998) Regional groundwater modelling of the Sherwood Sandstone Aquifer in the Lagan Valley
- Klingbeil R, Kleineidam S, Aspiron U, Aigner T, Teutsch G (1999) Relating lithofacies to hydrofacies: outcrop-based hydrogeological characterisation of Quaternary gravel deposits. *Sediment Geol* 129(3–4):299–310. doi:10.1016/S0037-0738(99)00067-6
- Lochbühler T, Pirot G, Straubhaar J, Linde N (2014) Conditioning of multiple-point statistics facies simulations to tomographic images. *Math Geosci* 46:625–645. doi:10.1007/s11004-013-9484-z
- Lyle P (1980) A petrological and geochemical study of the Tertiary Basaltic rocks of Northeast Ireland. *J Earth Sci Roy Dublin Soc* 2(2):137–152
- Manning PI, Robbie JH, Wilson HE (1970) *Geology of Belfast and the Lagan Valley: memoir for 1:63360 geological sheet 36 (Northern Ireland)*, 2nd edn. H. M. Stationery Office, Belfast
- Mariethoz G, Renard P (2010) Reconstruction of incomplete data sets or images using direct sampling. *Math Geosci* 42:245–268. doi:10.1007/s11004-010-9270-0
- Mariethoz G, Renard P, Straubhaar J (2010) The direct sampling method to perform multiple-point geostatistical simulations. *Water Resour Res* 46(11), W11536. doi:10.1029/2008WR007621
- Matheron G (1962) *Traité de géostatistique appliquée [Treaty of applied geostatistics]*. Technip, Paris
- Matheron G (1965) *Les variables régionalisées et leur estimation: une application de la théorie des fonctions aléatoires aux sciences de la nature [Regionalized variables and their estimation: an application of the theory of random functions for natural sciences]*. Masson, Paris
- Matheron G (1967) *Eléments pour une théories des milieux poreux [Elements for a theory of porous media]*. Masson, Paris
- McCabe M (2008) *Glacial geology and geomorphology: the landscapes of Ireland*. Dunedin Academic, Edinburgh, 274 pp
- McNeill GW, Cronin AA, Yang Y, Elliot T, Kalin RM (2000) The Triassic Sherwood Sandstone aquifer in Northern Ireland: constraint of a groundwater flow model for resource management. In: Robins NS, Misstear BD (eds) *Groundwater in The Celtic regions: studies in hard rock and Quaternary hydrogeology*. The Geological Society, London, pp 179–190
- Meerschman E, Pirot G, Mariethoz G, Straubhaar J, Van Meirvenne M, Renard P (2013) A practical guide to performing multiple-point statistical simulations with the direct sampling algorithm. *Comput Geosci* 52:307–324. doi:10.1016/j.cageo.2012.09.019
- Meerschman E, Van Meirvenne M, Mariethoz G, Islam MM, de Smedt P, Van de Vijver E, Saey T (2014) Using bivariate multiple-point statistics and proximal soil sensor data to map fossil ice-wedge polygons. *Geoderma* 213:571–577. doi:10.1016/j.geoderma.2013.01.016
- Michael HA, Li H, Boucher A, Sun T, Caers J, Gorelick SM (2010) Combining geologic-process models and geostatistics for conditional simulation of 3-D subsurface heterogeneity. *Water Resour Res* 46, W05527. doi:10.1029/2009WR008414

- Noetinger B, Artus V, Zargar G (2005) The future of stochastic and upscaling methods in hydrogeology. *Hydrogeol J* 13:184–201. doi:10.1007/s10040-004-0427-0
- Okazaki K, Mogi T, Utsugi M, Ito Y, Kunishima H, Yamazaki T, Takahashi Y, Hashimoto T, Yamaya Y, Ito H, Kaieda H, Tsukuda K, Yuuki Y, Jomori A (2011) Airborne electromagnetic and magnetic surveys for long tunnel construction design. *Phys Chem Earth* 36(16):1237–1246. doi:10.1016/j.pce.2011.05.008
- Pirot G, Renard P, Straubhaar J (2014) Simulation of braided river elevation model time series with multiple-point statistics. *Geomorphology* 214:148–156. doi:10.1016/j.geomorph.2014.01.022
- Rasmussen P, Sonnenborg TO, Gonciar G, Hinsby K (2013) Assessing impacts of climate change, sea level rise, and drainage canals on saltwater intrusion to coastal aquifer. *Hydrol Earth Syst Sci* 17:421–443. doi:10.5194/hess-17-421-2013
- Remy N, Boucher A, Wu J (2009) Applied geostatistics with SGeMS: a user's guide. Cambridge University Press, New York, 264 pp
- Renard P (2007) Stochastic hydrogeology: what professionals really need? *Ground Water* 45(5):531–541. doi:10.1111/j.1745-6584.2007.00340.x
- Renard P, de Marsily G (1997) Calculating equivalent permeability: a review. *Adv Water Resour* 5–6:253–278. doi:10.1016/S0309-1708(96)00050-4
- Rezaee H, Mariethoz G, Koneshloo M, Asghari O (2013) Multiple-point geostatistical simulation using the bunch-pasting direct sampling method. *Comput Geosci* 54:293–308. doi:10.1016/j.cageo.2013.01.020
- Rezaee H, Asghari O, Koneshloo M, Ortiz JM (2014) Multiple-point geostatistical simulation of dykes: application at Sungun porphyry copper system, Iran. *Stoch Environ Res Risk Assess.* doi:10.1007/s00477-014-0857-8
- Robins NS (1996) Hydrogeology of Northern Ireland. Environment and Heritage Service, HMSO for the British Geological Society, London, 60 pp
- Rubin Y, Hubbard SS (eds) (2005) Hydrogeophysics, vol 50. In: Water science and technology library, Springer, Dordrecht, The Netherlands, 523 pp
- Straubhaar J, Renard P, Mariethoz G, Froidevaux R, Besson O (2011) An improved parallel multiple-point algorithm using a list approach. *Math Geosci* 43:305–328. doi:10.1007/s11004-011-9328-7
- Strebelle S (2001) Sequential simulation drawing structures from training images. PhD Thesis, Stanford University, Stanford, CA
- Strebelle S (2002) Conditional simulation of complex geological structures using multiple-point statistics. *Math Geol* 34(1):1–22
- Sulzbacher H, Wiederhold H, Siemon B, Grinat M, Igel J, Burschil T, Günther T, Hinsby K (2012) Numerical modelling of climate change impacts on freshwater lenses on the North Sea Island of Borkum using hydrological and geophysical methods. *Hydrol Earth Syst Sci* 16:3621–3642. doi:10.5194/hess-16-3621-2012
- Virdee TS, Kottegoda NT (1984) A brief review of kriging and its application to optimal interpolation and observation well selection. *Hydrol Sci J* 29(4):367–387. doi:10.1080/0262668409490957
- Wen X-H, Gómez-Hernández JJ (1996) Upscaling hydraulic conductivities in heterogeneous media: an overview. *J Hydrol* 183(1–2):9–32. doi:10.1016/S0022-1694(96)80030-8
- Whitehouse NJ, Roe HM, McCarron S, Knight J (eds) (2008) North of Ireland: field guide. Quaternary Research Association, London, 286 pp
- Wilson RL (1959) Remanent magnetism of late Secondary and early Tertiary igneous rocks. *Philos Mag* 4:750–755. doi:10.1080/14786435908243271
- Wilson RL (1970) Palaeomagnetic stratigraphy of Tertiary lavas from Northern Ireland. *Geophys J R Astron Soc* 20:1–9. doi:10.1111/j.1365-246X.1970.tb06744.x
- Wilson HE (1972) Regional geology of Northern Ireland. HMSO, Belfast, 115 pp
- Wilson C (2011) Analysis of the effect of volcanic dykes on groundwater flow in the Sherwood Sandstone aquifer: impacts on piezometry, salinity, and attenuation of the tidal signal. MSc Thesis, Queen's Univ., Belfast, Ireland
- Yang YS, Cronin AA, Elliot T, Kalin RM (2004) Characterising a heterogeneous hydrogeological system using groundwater flow and geochemical modelling. *J Hydraul Res* 42:147–155. doi:10.1080/00221680409500058